NATIONAL ADVISORY COMMITTEE FOR AERONAUTICS

TECHNICAL NOTE 2080

WIND-TUNNEL INVESTIGATION AT LOW SPEED OF AN UNSWEPT

UNTAPERED SEMISPAN WING OF ASPECT RATIO 3.13

EQUIPPED WITH VARIOUS 25-PERCENT-

CHORD PLAIN FLAPS

By Harold S. Johnson and John R. Hagerman

Langley Aeronautical Laboratory
Langley Air Force Base, Va.

NACA

Washington

April 1950

20000801 091

DTIC QUALITY INSPECTED 4

AQM00-10-3370

NATIONAL ADVISORY COMMITTEE FOR AERONAUTICS

TECHNICAL NOTE 2080

WIND-TUNNEL INVESTIGATION AT LOW SPEED OF AN UNSWEPT

UNTAPERED SEMISPAN WING OF ASPECT RATIO 3.13

EQUIPPED WITH VARIOUS 25-PERCENT-

CHORD PLAIN FLAPS

By Harold S. Johnson and John R. Hagerman

SUMMARY

Force and moment data were obtained at low speeds to determine the aerodynamic characteristics of an unswept untapered semispan wing of NACA 64A010 section and aspect ratio 3.13 equipped with 25-percent-chord unsealed plain flaps having various spans and spanwise locations. Lift, drag, pitching-moment, and flap hinge-moment data were obtained for the wing with the various flaps deflected up to 60°.

In general, changes in angle of attack, flap deflection, or flap span and spanwise location produced trends in lift, drag, pitching moment, and flap hinge moment that were similar to but of different magnitudes from those for unswept wings of higher aspect ratio. The increment of lift coefficient due to 30° of flap deflection was relatively unaffected by the spanwise location of the flaps and increased nearly linearly with flap span. Because of the increase in the drag coefficients and the associated decrease in the values of the lift-drag ratio with increasing flap deflection, an advantage may be gained by limiting the flap deflection to moderate angles (about 30°), even though the lift coefficients increase with further increases in flap deflection.

INTRODUCTION

The National Advisory Committee for Aeronautics is conducting an extensive investigation of the lift and control effectiveness of various flaps and control surfaces on wings having plan forms suitable for transonic and supersonic airplanes. The ultimate objective is to obtain flap and aileron design criterions similar to those available for wings of conventional low-speed plan forms (references 1 to 6).

As part of this broad study, the lift and lateral control character-
istics of an untapered low-aspect-ratio semispan wing having various
amounts of sweep and equipped with 25-percent-chord unsealed plain
flaps or ailerons having various spans and spanwise locations are being
investigated in the Langley 300 MPH 7- by 10-foot tunnel.

This paper presents the results of the investigation of the
unswept wing configuration having an aspect ratio of 3.13 and utilizing
the 25-percent-chord control surfaces as lift flaps. Lift, drag,
pitching-moment, and flap hinge-moment data were obtained through an
angle-of-attack range for various flap deflections up to 60°.

SYMBOLS

The forces and moments measured on the wing are presented about
the wind axes which, for the conditions of these tests (zero yaw),
correspond to the stability axes. The lift, drag, and pitching-moment
data are presented about the point shown in figure 1 which corresponds
to the 25-percent-chord station of the mean aerodynamic chord.

C_L lift coefficient (L/qS)

ΔC_L increment of lift coefficient

C_D drag coefficient (D/qS)

C_m pitching-moment coefficient $(M/qS\bar{c})$

ΔC_m increment of pitching-moment coefficient

C_h flap hinge-moment coefficient $(H/2qM_1)$

L twice lift of semispan model, pounds

D twice drag of semispan model, pounds

M twice pitching moment of semispan model measured about $0.25\bar{c}$,
                foot-pounds

H flap hinge moment, measured about flap hinge axis, foot-pounds

M_1 area moment of flap rearward of and about hinge axis, cubic
                feet (see table I)

q free-stream dynamic pressure, pounds per square foot $\left(\frac{1}{2}\rho V^2\right)$

S   twice area of semispan wing model, 19.16 square feet

b   twice span of semispan model, 7.750 feet

$\bar{c}$ wing mean aerodynamic chord, 2.500 feet

c   local chord, feet

y   lateral distance from plane of symmetry, feet

b_f span of flap, feet

V   free-stream velocity, feet per second

ρ mass density of air, slugs per cubic foot

α angle of attack of wing with respect to chord plane at root of model, degrees

δ_f flap deflection relative to wing chord plane, measured perpendicular to flap hinge axis (positive when trailing edge is down), degrees

$$C_{L_\delta} = \left(\frac{\partial C_L}{\partial \delta_f}\right)_\alpha$$

$$C_{L_\alpha} = \left(\frac{\partial C_L}{\partial \alpha}\right)_{\delta_f}$$

$$\alpha_\delta = \frac{C_{L_\delta}}{C_{L_\alpha}}$$

The subscripts outside the parentheses indicate the factor held constant. The parameters were measured in the vicinity of 0° angle of attack or 0° flap deflection.

Subscripts:

f   flap

f_i inboard end of flap

f_o outboard end of flap

max   maximum

The lift, drag, and pitching-moment-coefficient data presented herein represent the aerodynamic effects of deflection of the flaps in the same direction on both semispans of the complete wing.

CORRECTIONS

Jet-boundary corrections, determined by the method presented in reference 7, have been applied to the angle-of-attack and drag-coefficient values. Blockage corrections, to account for the constriction effects of the model and its wake, have also been applied to the test data (reference 8). No corrections have been applied to the data to account for the very small amount of wing twist produced by flap deflection or for the effect of air-flow leakage around the end plate at the root of the model.

MODEL AND APPARATUS

The semispan-wing model used in the investigation was constructed of laminated mahogany over a solid-steel spar. The plan-form dimensions are shown in figure 1. The wing sections were NACA 64A010 and the model had 0° sweepback, an aspect ratio of 3.13 (based on full-span dimensions), and a taper ratio of 1.0. The wing model had neither twist nor dihedral. A cross section of the wing showing the details of the 25-percent-chord radius-nose unsealed plain flaps is shown in figure 1. The flaps were constructed of mahogany with steel spars and had joints at three span-wise stations so that various spans of flaps at various spanwise locations could be investigated (fig. 1 and table I). The chordwise gaps between flap segments were sealed when two or more flap segments were tested in combination. A motor-driven flap-actuating mechanism which was remotely controlled was used to obtain the various flap deflections used in the investigation, and these deflections were constantly indicated on a meter by the use of a calibrated potentiometer which was mounted on the hinge axis near the root chord of the model. The flap hinge moments were measured by a calibrated electrical resistance type of strain gage.

The semispan-wing model was mounted vertically in the Langley 300 MPH 7- by 10-foot tunnel with the root chord adjacent to the ceiling of the tunnel, which served as a reflection plane (fig. 2). The model was mounted on the six-component balance system so that all forces and moments acting on the model could be measured. A small clearance was maintained between the model and the tunnel ceiling so that no part of the model came into contact with the tunnel structure. A $\frac{1}{16}$-inch-thick

metal end plate was attached to the root of the model to deflect the air flowing into the test section through the clearance hole in order to minimize the effect of this spanwise air flow on the flow over the model.

The Langley 300 MPH 7- by 10-foot tunnel is a closed-throat single-return tunnel. Measurements have indicated that the turbulence factor is very close to unity.

TESTS

All the tests were performed at an average dynamic pressure of approximately 100 pounds per square foot, which corresponds to a Mach number of 0.27 and a Reynolds number of about 4.5×10^6 based on the wing mean aerodynamic chord of 2.500 feet.

Tests with the inboard half-span and the full-span flaps deflected at seven deflections between 0° and 60° were performed through an angle-of-attack range from -4° through the wing stall. The additional data for other spans and spanwise locations presented herein were obtained in the course of obtaining lateral-control test data.

RESULTS AND DISCUSSION

The static aerodynamic characteristics of the wing in pitch for seven deflections of the inboard half-span and the full-span flaps are presented in figures 3 and 4, respectively. Corresponding data for the wing equipped with outboard flaps having various spans and for the wing equipped with half-span flaps at various spanwise locations are presented in figures 5 and 6, respectively, for a flap deflection of 30°. The incremental values of lift and pitching-moment coefficients resulting from flap deflection are shown in figures 7 and 8, respectively. The effects of flap span and spanwise location on the lift and pitching-moment coefficients for the wing at $\delta_f = 30^\circ$ are presented in figures 9 and 10, respectively. Figure 11 presents a comparison of the experimental and estimated lift-effectiveness parameters for the model equipped with both inboard and outboard flaps. The experimental data for the outboard flaps were obtained in the course of obtaining lateral-control test data.

Lift characteristics.- For the angle-of-attack range covered in the investigation, increasing either the flap span or the flap deflection resulted in an increase in the lift at any given angle of attack and

also resulted in an increase in the maximum lift obtainable, except for
the model with the inboard half-span and the full-span flaps deflected 60°
for which a slight decrease in $C_{L_{max}}$ was obtained as the flap deflec-
tion was increased from 50° to 60°. The incremental lift produced by
unit flap deflection generally decreased as the flap deflection or
angle of attack was increased; however, at low angles of attack, the
wing with the full-span flaps deflected 50° and 60° exhibited larger
increments of lift produced by unit flap deflection than was exhibited
at a deflection of 40° (figs. 3, 4, and 7). As will be discussed later,
the hinge-moment data for the outboard $0.242\frac{b}{2}$ flap (presented for
$\delta_f = 30^O$ in fig. 5) and the hinge-moment and pitching-moment data for
both the inboard half-span and the full-span flaps (figs. 3 and 4, respec-
tively) indicate that a region of high loading was located at the trailing
edge of the wing near the tip at large effective angles of attack. This
region of high loading was apparently accentuated by large deflections
of the full-span flap, thereby producing the aforementioned increase in
effectiveness of the flap at large deflections. A similar loading dis-
tribution was noted for the unflapped rectangular wings of reference 9
at high angles of attack.

The values of ΔC_L (fig. 7) obtained with the inboard half-span
and the full-span flaps deflected 30° and 60° are summarized in the
following table:

Flap span, $\dfrac{b_f}{b/2}$	δ_f (deg)	ΔC_L		$\Delta C_{L_{max}}$
		$\alpha = 0^O$	$\alpha = 12^O$	
0.484	30	0.37	0.33	0.27
.484	60	.50	.43	.30
.968	30	.67	.61	.49
.968	60	.90	.69	.52

The increments of C_L are lower at $C_{L_{max}}$ than at a constant angle of
attack mainly because a larger portion of the wing is stalled at $C_{L_{max}}$
when the flaps are deflected to large angles. The usual reduction
in ΔC_L and $\Delta C_{L_{max}}$ with decreasing aspect ratio is shown when the
values are compared with those for the aspect-ratio-6 rectangular wing
of reference 1 (accounting for the differences in flap chord on the
basis of three-dimensional data at higher aspect ratios).

The effects of flap span and spanwise location on the lift effectiveness (figs. 3 to 6) are summarized in figure 9 for the various flap spans tested at a flap deflection of 30° and at angles of attack of 0° and 12°. These data show that the lift produced by flaps of corresponding percent span was relatively unaffected by spanwise location, whereas a study of figure 11 indicates that, for the low values of flap deflection where the values of C_{L_δ} are measured, the inboard flaps are more effective in producing lift than flaps with outboard locations. The flaps having inboard locations lose effectiveness at a more rapid rate with increasing flap deflection than do the flaps having outboard locations. Results of other investigations (references 1 and 2) of wings having higher aspect ratios have indicated that inboard flaps are more effective throughout the flap-deflection range than flaps covering outboard portions of the span. Figures 3 to 5 and 9 also show that the lift coefficient increased almost linearly with increasing flap span and that this relationship was relatively unaffected by changes in angle of attack below $\alpha = 12°$.

The value of C_{L_α} (with the flaps undeflected) was approximately 0.055. The experimental values of C_{L_δ} at $\alpha = 0°$ were about 0.016 and 0.030 for the inboard half-span and the full-span flaps, respectively, and decreased only slightly at the higher angles of attack. Estimated values of the lift-effectiveness parameter C_{L_δ} were computed by method I of reference 10 for the four spans of outboard flaps tested and by an application of the Weissinger method for inboard-flap locations. The value of α_δ from section data for the NACA 64A010 airfoil equipped with an unsealed flap type of control (reference 11), corrected to $\frac{c_f}{c} = 0.25$ by the method of reference 10, was used in the computations of C_{L_δ}. This value of α_δ was considerably higher than the value of α_δ obtained from the general curves of references 6 and 10. A comparison of the experimental and estimated values of the lift-effectiveness parameter is presented in figure 11 and shows very good agreement. The experimental C_{L_δ} values for the outboard flaps were obtained from the unpublished lateral-control data.

A comparison with the model of reference 12, which had the same airfoil section, sweep, and aspect ratio but had a taper ratio of 0.5, showed that the experimental C_{L_δ} for the model with full-span flaps was slightly higher than that for the model of reference 12 corrected to $\frac{c_f}{c} = 0.25$.

Drag characteristics.- Analysis of the drag data shows that increases in the flap span or flap deflection increased the values of drag coefficient for all angles of attack below $\alpha = 12^{\circ}$ (figs. 3 to 5). A comparison of the lift-drag ratios L/D for the wing with both the inboard half-span and the full-span flaps indicates that the L/D ratio decreases as the flap deflection is increased, with a flap deflection of 30° providing almost the optimum value of L/D for lift coefficients greater than about 1.0. As will be discussed in the following section, an advantage gained by limiting the flap deflection to moderate angles is the smaller longitudinal-trim change resulting from flap deflection.

A study of figure 6 reveals that the drag coefficient increased slightly as the half-span flap was moved outboard on the wing. This increase in C_D is attributed to the region of the high loading located at the trailing edge of the wing near the tip at large effective angles of attack as previously noted.

Pitching-moment characteristics.- For all flap configurations and flap deflections, the wing had an unstable variation of pitching-moment coefficient with lift coefficient and the aerodynamic center was located at about $0.20\bar{c}$ (figs. 3 to 6). This longitudinal instability generally decreased as the lift coefficient was increased, although at the highest flap deflections (50° and 60°) C_m varied erratically with C_L. Increases in either flap span or flap deflection produced negative increments of pitching-moment coefficient ΔC_m over the entire lift-coefficient range except at the highest flap deflections (50° and 60°) where ΔC_m produced by unit flap deflection decreased with an increase in flap deflection in the high angle-of-attack range (figs. 3 to 5 and 8). The values of ΔC_m varied linearly with flap deflection only for deflections of less than about 20° (fig. 8). For flap deflections greater than 20°, the ΔC_m values generally exhibited only a small increase with unit flap deflection. The data of figures 3 to 5 and 8 also indicate that the values of ΔC_m were relatively unaffected by angle-of-attack variations, except perhaps for the wing with the full-span flap at large flap deflections.

The data for the outboard flaps $\left(\dfrac{y_{f_0}}{b/2} = 0.968\right)$ indicate that the pitching-moment coefficient showed an almost linear variation with flap span (figs. 5 and 10). The pitching-moment coefficients due to flap deflection are greater for flaps with their outboard end at the tip than for inboard flaps of the same span (figs. 3 to 6 and 10) because of the high loading region located at the trailing edge of the wing near the tip.

<u>Hinge-moment characteristics</u>.- The flap hinge-moment data of figures 3 to 6 show, as would normally be expected, that the values of flap hinge-moment coefficient generally became more negative as both the flap deflection and the angle of attack were increased except for high deflections at inboard flap locations where the values of C_h became less negative with increasing α. (See fig. 3.) The hinge-moment coefficients of the outboard flaps generally became less negative as the flap span was increased and this decrease in C_h became less pronounced as the flap span approached full span (fig. 5). A similar decrease in magnitude in C_h due to spanwise location of the half-span flaps was noted when the flap was moved inboard from the wing tip (fig. 6).

These general trends of hinge-moment coefficient with flap span and spanwise location agree with the data of reference 9 which show a region of high loading located near the trailing edge at the wing tip of untapered low-aspect-ratio wings at high effective angles of attack.

CONCLUSIONS

A wind-tunnel investigation was performed at low speed to determine the aerodynamic characteristics of an unswept untapered semispan wing of aspect ratio 3.13 equipped with 25-percent-chord unsealed plain flaps having various spans and spanwise locations. The results of the investigation led to the following conclusions:

1. Changes in angle of attack, flap deflection, or flap span and spanwise flap location generally produced trends in lift, drag, pitching moment, and flap hinge moment that were similar to but of different magnitude from those for unswept wings of higher aspect ratio.

2. The increment of lift coefficient due to 30° of flap deflection increased almost linearly with increasing flap span and was relatively unaffected by the spanwise location of the flaps.

3. Because of the increase in the drag coefficients and the associated decrease in the values of the lift-drag ratio with increasing flap deflection, an advantage may be gained by limiting the flap deflection to moderate angles (about 30°), even though increases in lift coefficient result from further increases in flap deflection.
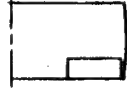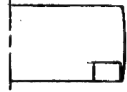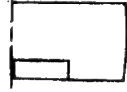

Langley Aeronautical Laboratory
        National Advisory Committee for Aeronautics
   Langley Air Force Base, Va., January 5, 1950

REFERENCES

1. House, R. O.: The Effects of Partial-Span Plain Flaps on the Aerodynamic Characteristics of a Rectangular and a Tapered Clark Y Wing. NACA TN 663, 1938.

2. House, Rufus O.: The Effects of Partial-Span Slotted Flaps on the Aerodynamic Characteristics of a Rectangular and a Tapered N.A.C.A. 23012 Wing. NACA TN 719, 1939.

3. Wenzinger, Carl J.: The Effects of Full-Span and Partial-Span Split Flaps on the Aerodynamic Characteristics of a Tapered Wing. NACA TN 505, 1934.

4. Weick, Fred E., and Jones, Robert T.: Résumé and Analysis of N.A.C.A. Lateral Control Research. NACA Rep. 605, 1937.

5. Pearson, Henry A., and Jones, Robert T.: Theoretical Stability and Control Characteristics of Wings with Various Amounts of Taper and Twist. NACA Rep. 635, 1938.

6. Langley Research Staff (Compiled by Thomas A. Toll): Summary of Lateral-Control Research. NACA Rep. 868, 1947.

7. Polhamus, Edward C.: Jet-Boundary-Induced-Upwash Velocities for Swept Reflection-Plane Models Mounted Vertically in 7- by 10-Foot, Closed, Rectangular Wind Tunnels. NACA TN 1752, 1948.

8. Herriot, John G.: Blockage Corrections for Three-Dimensional-Flow Closed-Throat Wind Tunnels, with Consideration of the Effect of Compressibility. NACA RM A7B28, 1947.

9. Norton, F. H., and Bacon, D. L.: Pressure Distribution over Thick Aerofoils - Model Tests. NACA Rep. 150, 1922.

10. Lowry, John G., and Schneiter, Leslie E.: Estimation of Effectiveness of Flap-Type Controls on Sweptback Wings. NACA TN 1674, 1948.

11. Dods, Jules B., Jr.: Wind-Tunnel Investigation of Horizontal Tails. IV - Unswept Plan Form of Aspect Ratio 2 and a Two-Dimensional Model. NACA RM A8J21, 1948.

12. Dods, Jules B., Jr.: Wind-Tunnel Investigation of Horizontal Tails. I - Unswept and 35° Swept-Back Plan Forms of Aspect Ratio 3. NACA RM A7K24, 1948.

TABLE I

DIMENSIONAL CHARACTERISTICS OF THE VARIOUS 0.25c FLAPS TESTED

ON THE WING HAVING AN ASPECT RATIO OF 3.13

Configuration	Flap span, $\dfrac{b_f}{b/2}$	Flap spanwise location		M_1 (cu ft)
		$\dfrac{y_{f_i}}{b/2}$	$\dfrac{y_{f_o}}{b/2}$	
	0.968	0	0.968	0.7324
	.726	.242	.968	.5493
	.484	.484	.968	.3662
	.242	.726	.968	.1831
	.484	.242	.726	.3662
	.484	0	.484	.3662
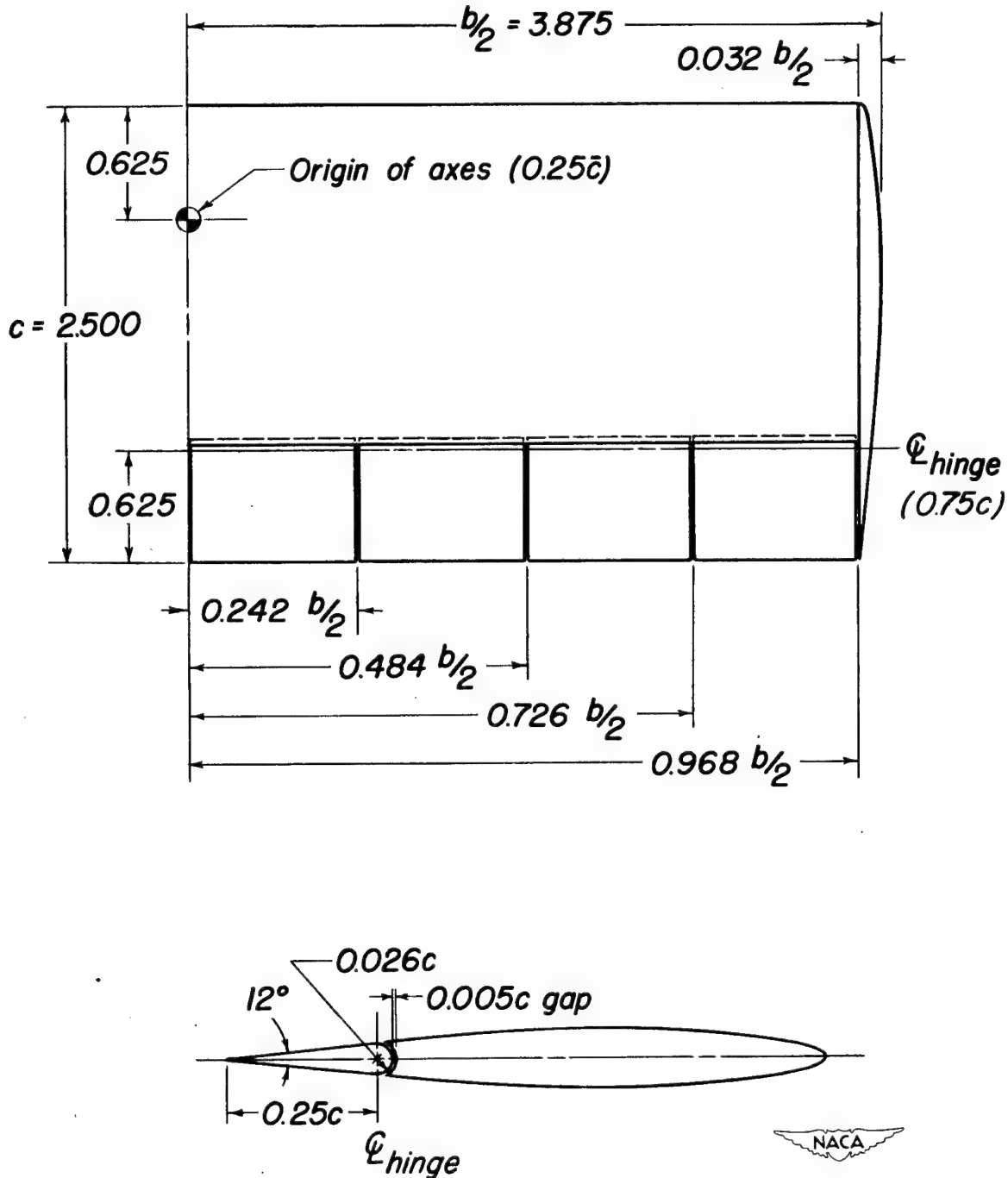
NACA

Figure 1.- Drawing of the unswept semispan-wing model having an aspect
ratio of 3.13. (All dimensions are in ft.)
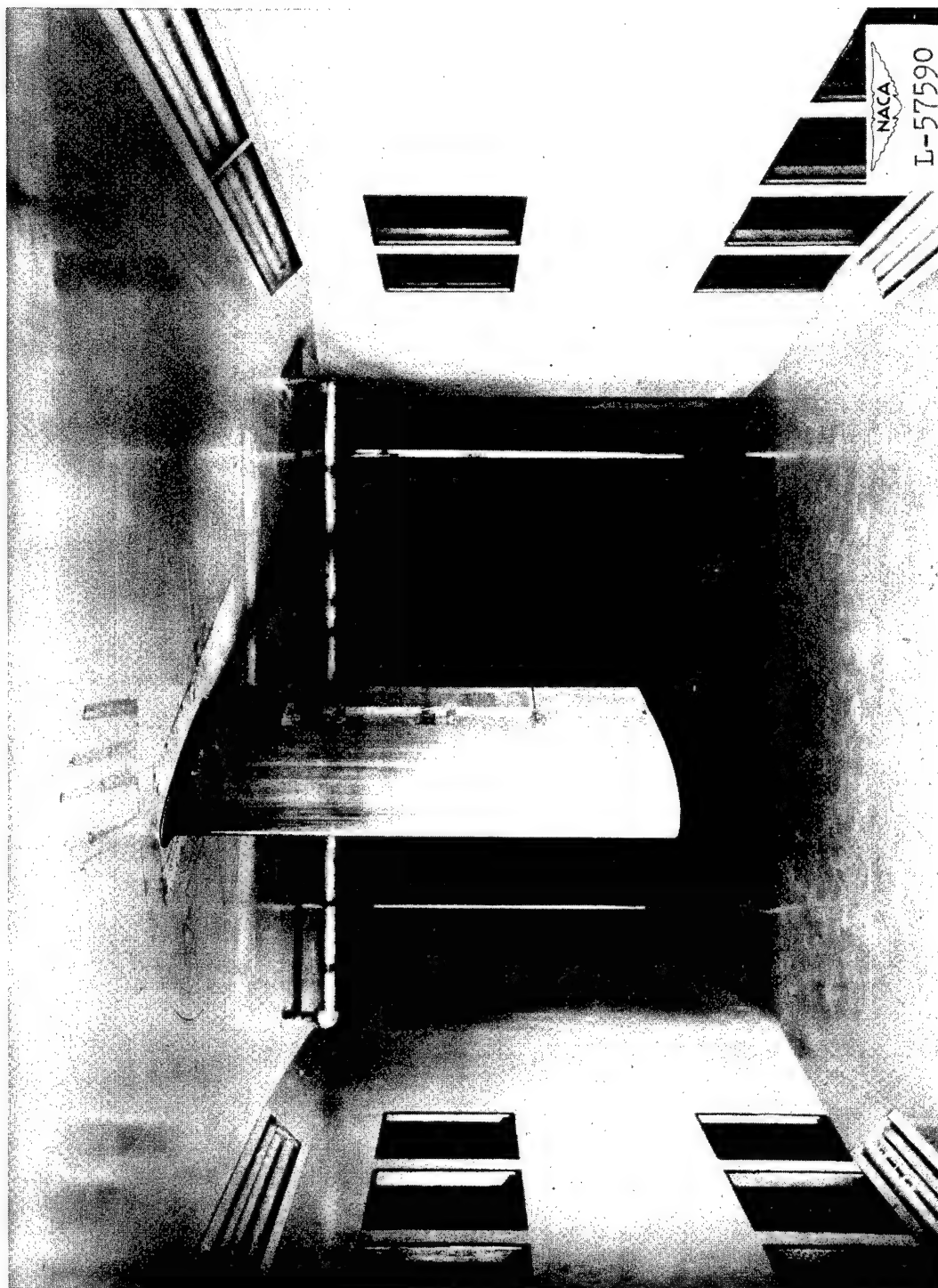
Figure 2.- Unswept semispan-wing model of aspect ratio 3.13 mounted in the Langley 300 MPH 7- by 10-foot tunnel.
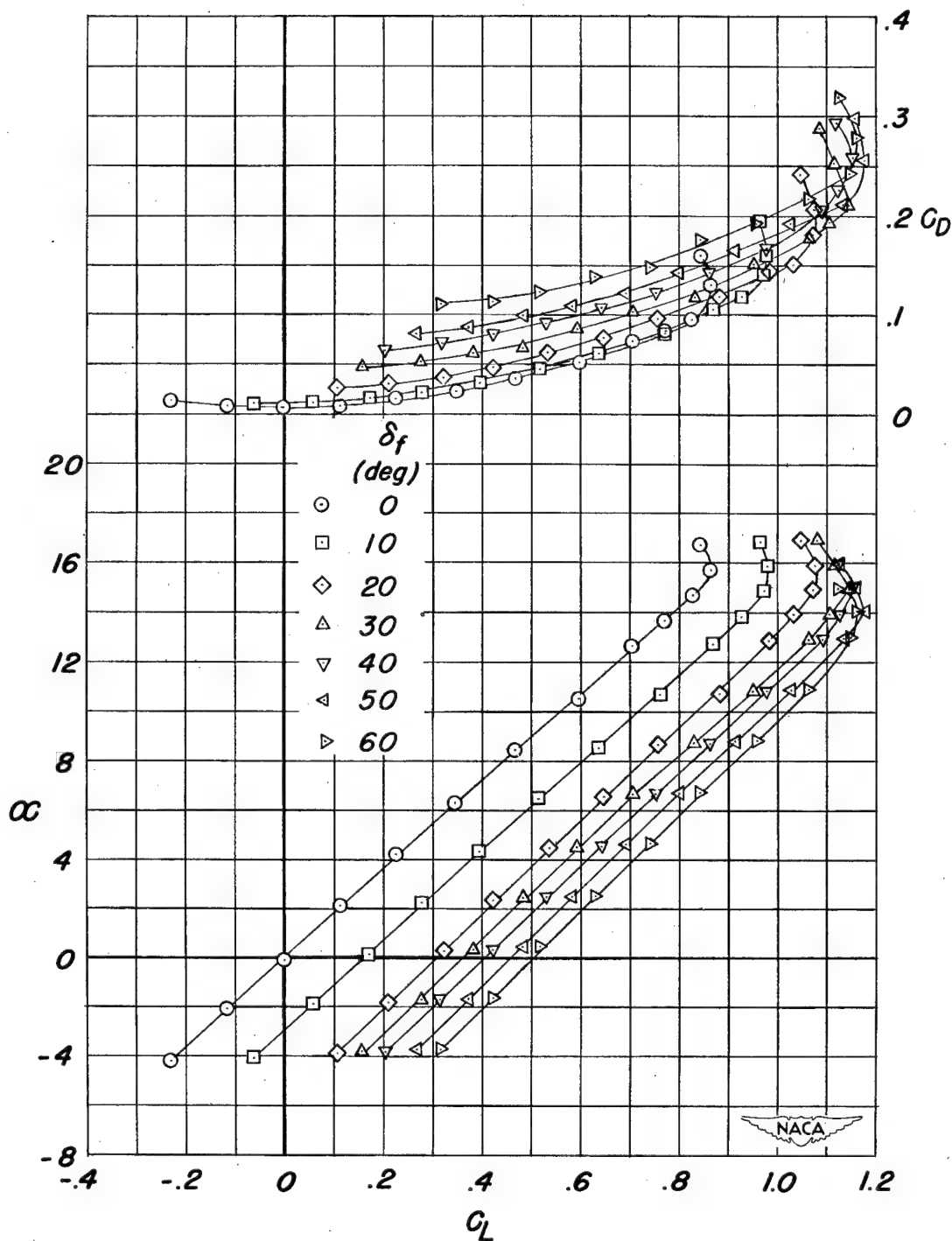
Figure 3.- Effect of flap deflection on the aerodynamic characteristics in pitch of the unswept wing of aspect ratio 3.13 equipped with inboard half-span flaps $\left(b_f = 0.484\frac{b}{2}\right)$. $y_{f_i} = 0$; $y_{f_o} = 0.484\frac{b}{2}$.
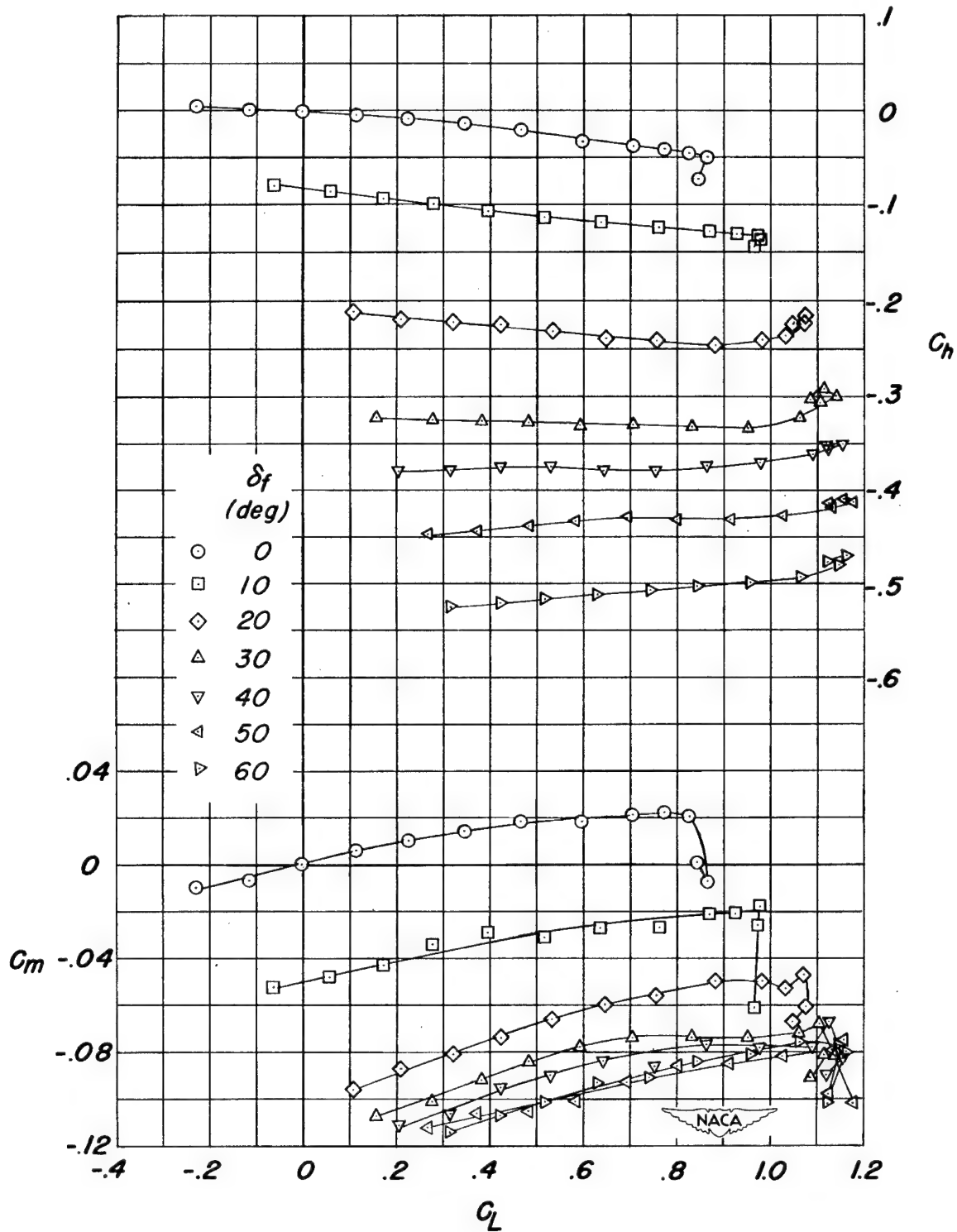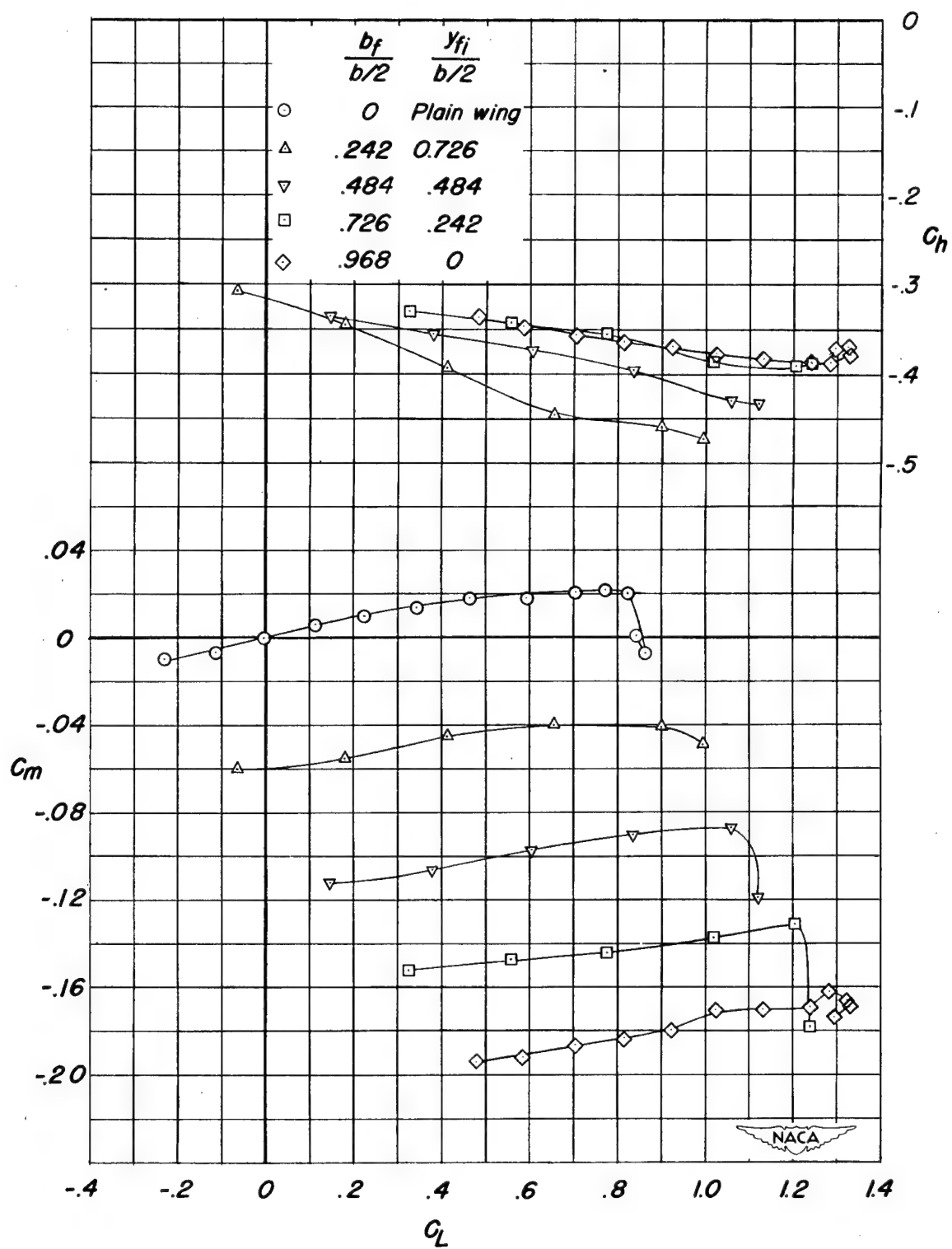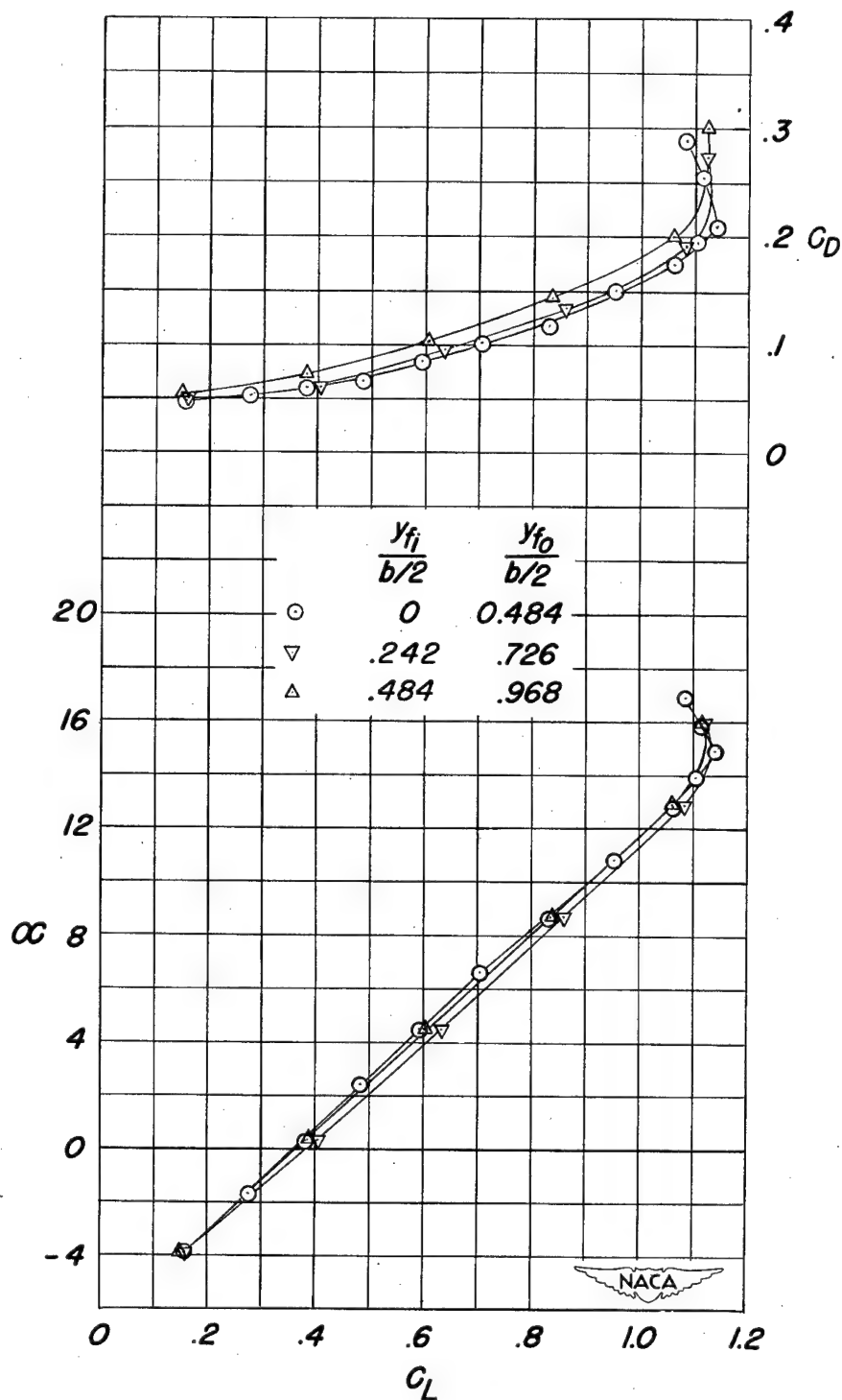
Figure 3.- Concluded.
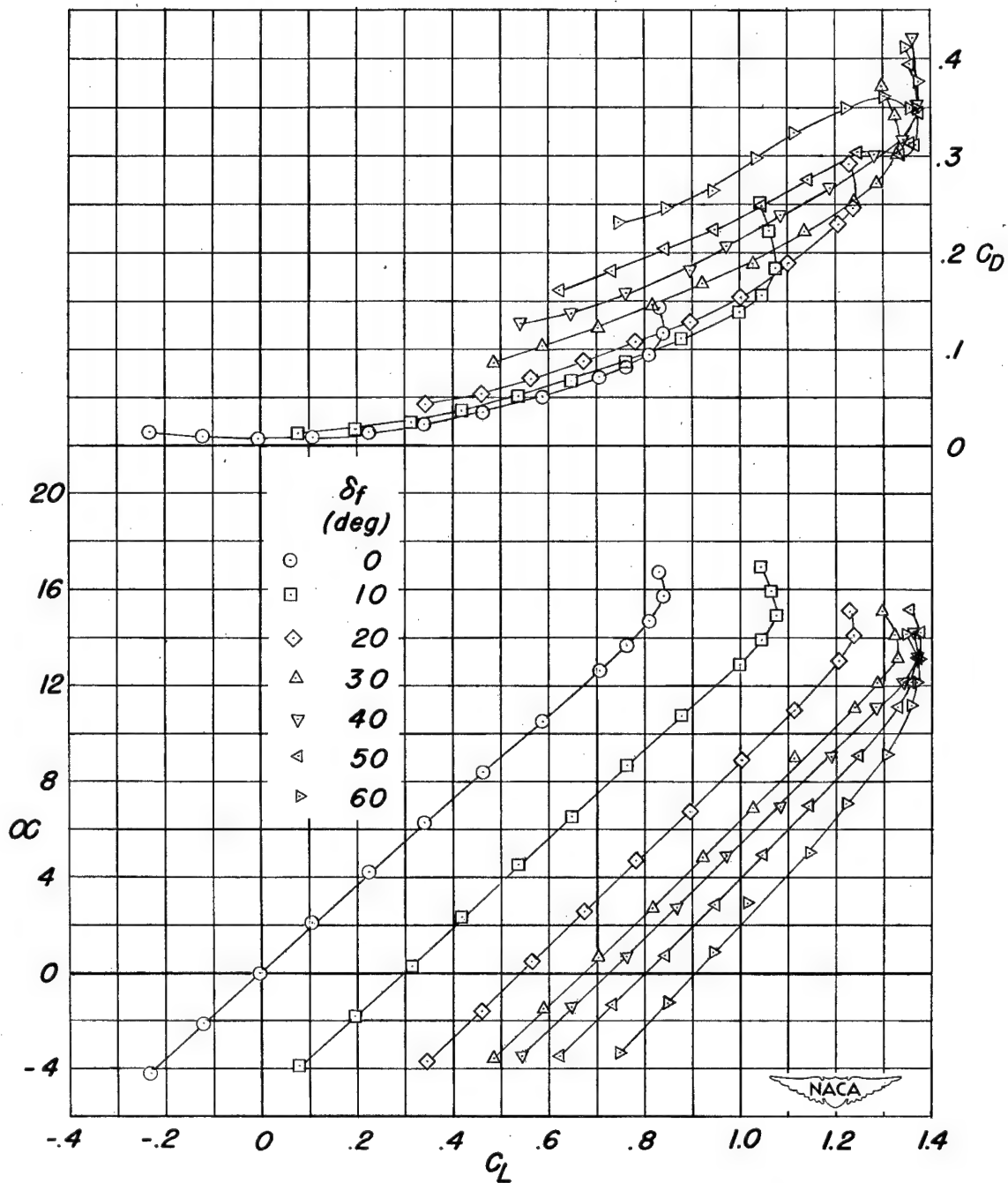
Figure 4.- Effect of flap deflection on the aerodynamic characteristics in pitch of the unswept wing of aspect ratio 3.13 equipped with full-span flaps $\left(b_f = 0.968\frac{b}{2}\right)$. $y_{f_i} = 0$; $y_{f_o} = 0.968\frac{b}{2}$.
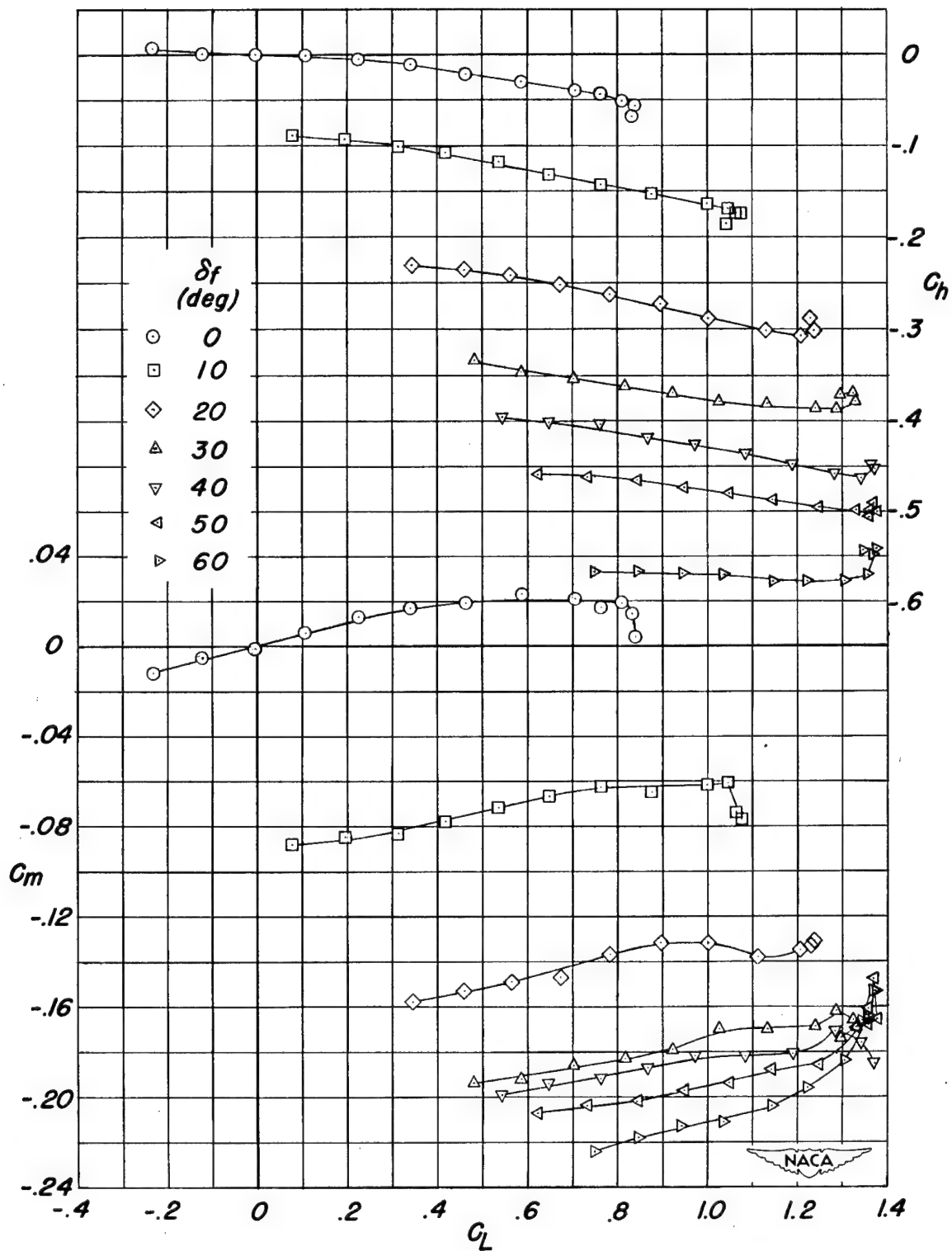
Figure 4.- Concluded.
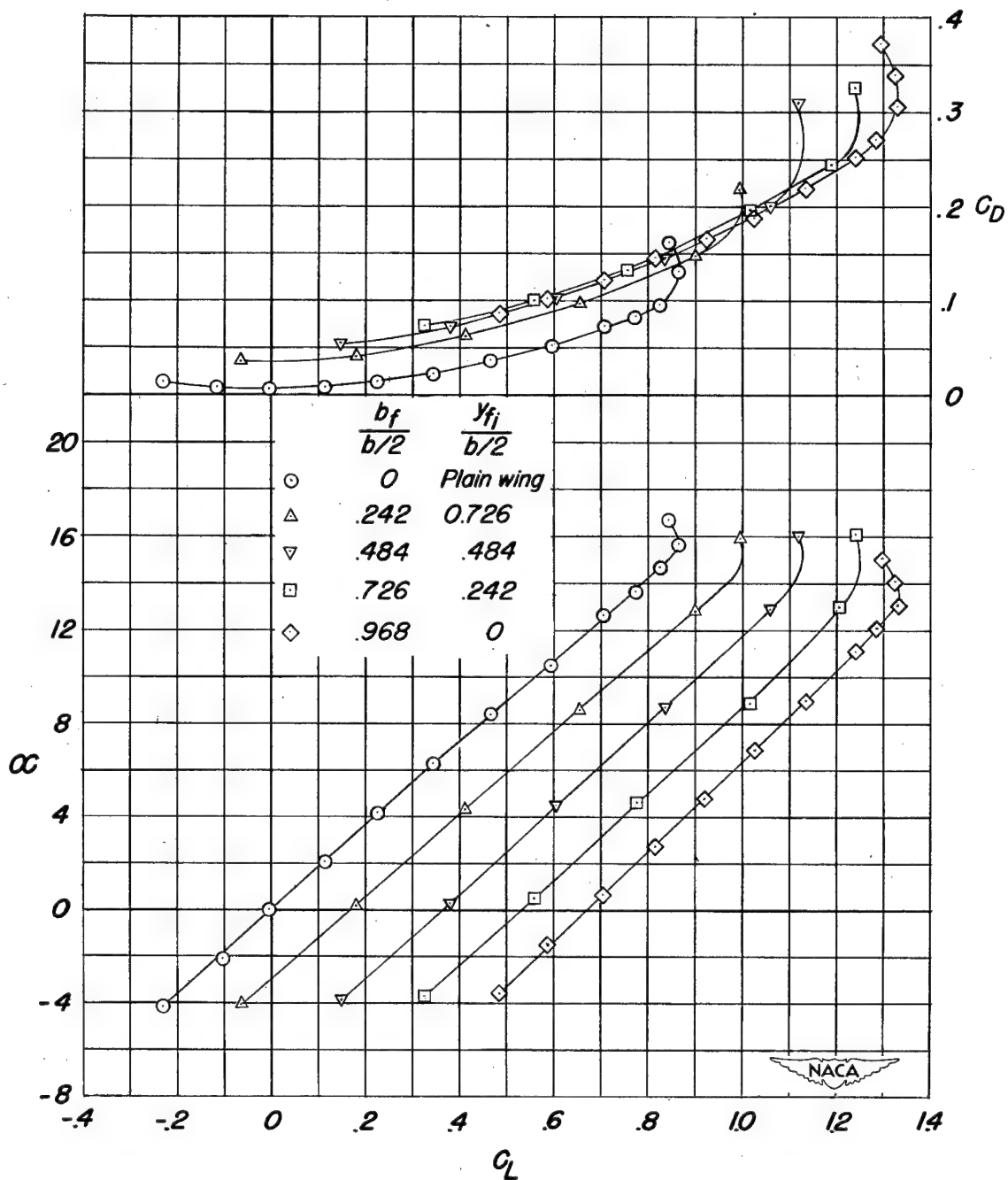
Figure 5.- Effect of flap span on the aerodynamic characteristics in pitch of the unswept wing of aspect ratio 3.13 equipped with outboard flaps $\left(y_{f_o} = 0.968 \frac{b}{2}\right)$. $\delta_f = 30^\circ$.

Figure 5.- Concluded.

Figure 6.- Effect of spanwise flap location on the aerodynamic characteristics in pitch of the unswept wing of aspect ratio 3.13 equipped with half-span flaps $\left(b_f = 0.484\frac{b}{2}\right)$. $\delta_f = 30^\circ$.
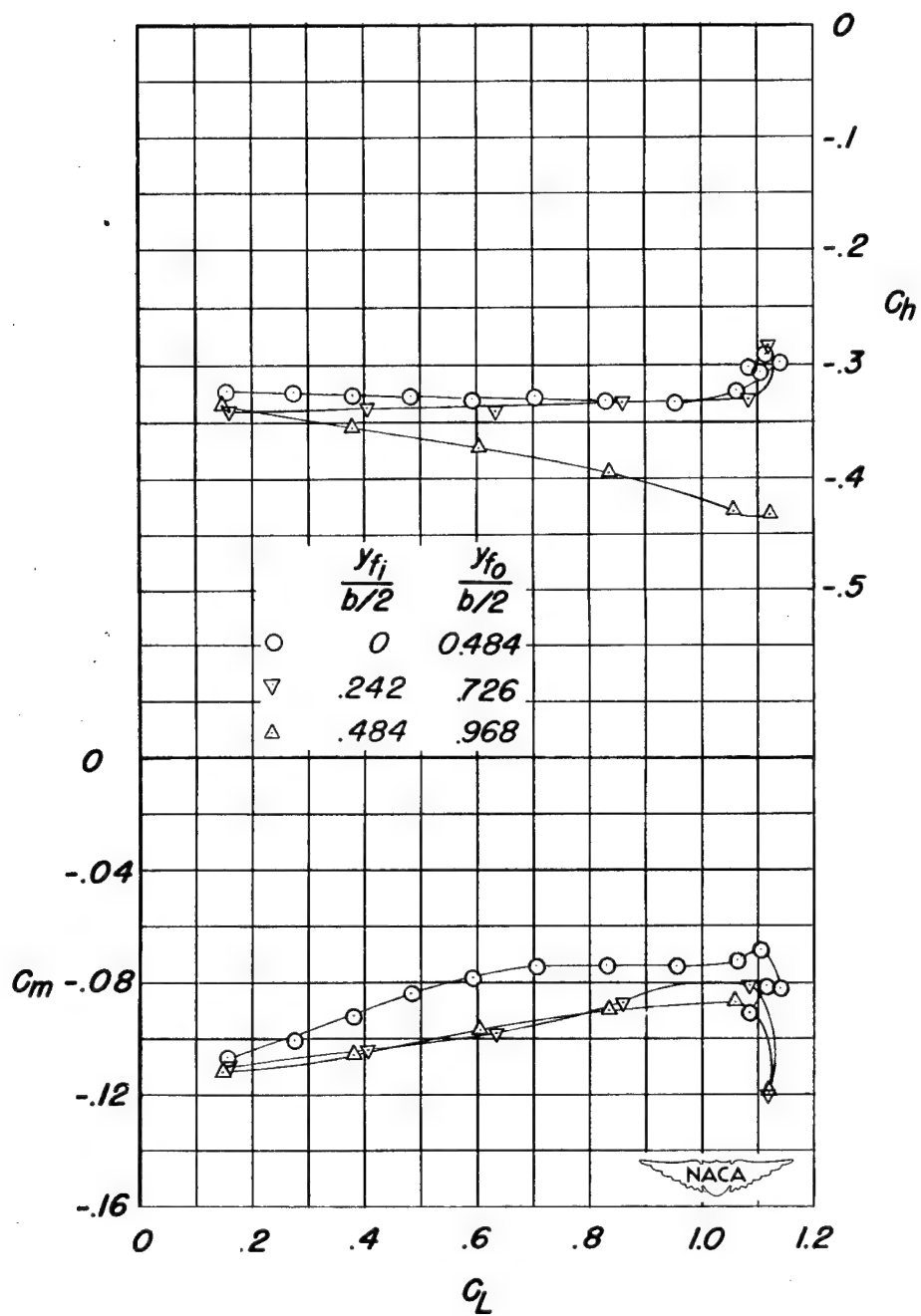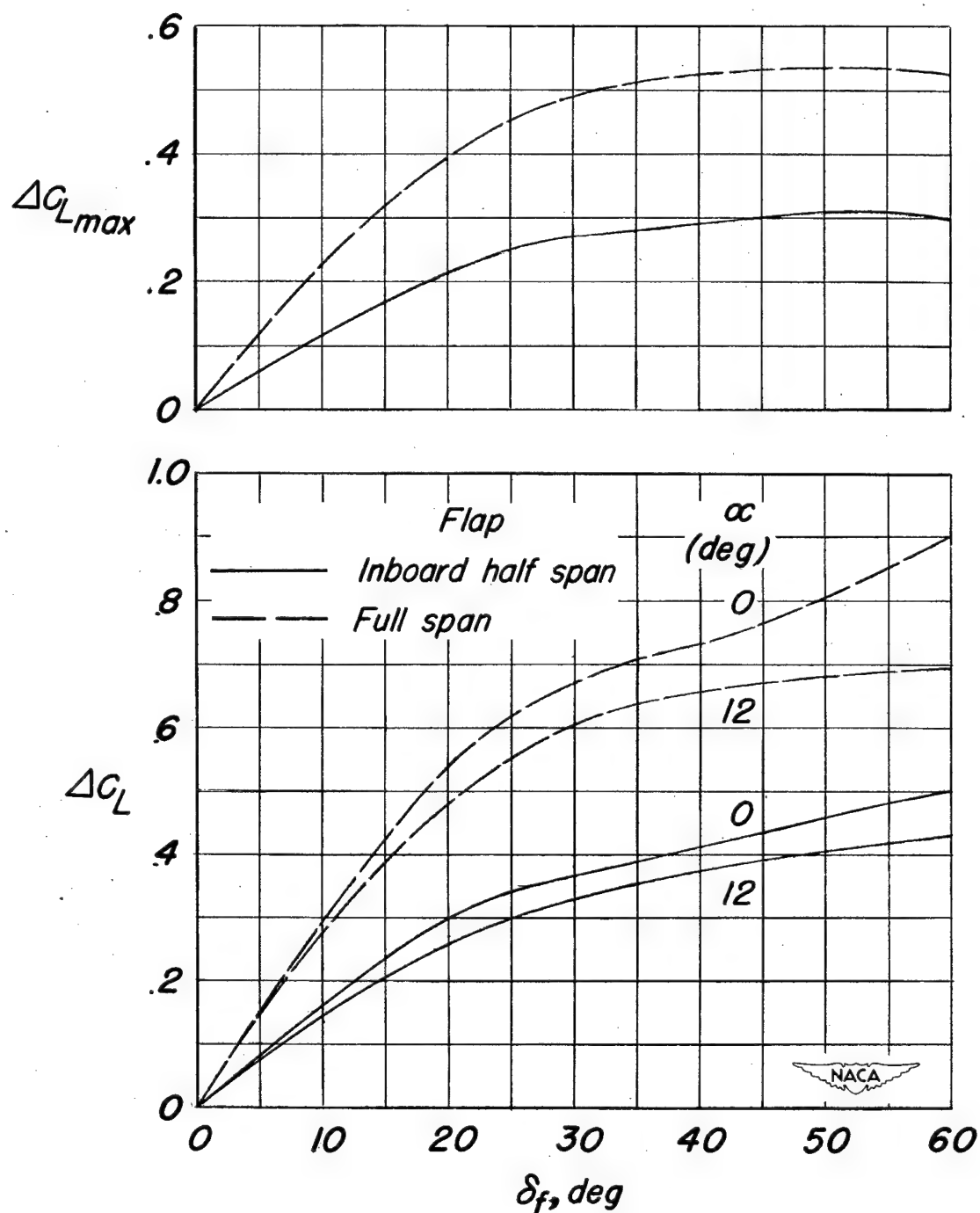
Figure 6.- Concluded.

Figure 7.- Variation of incremental lift coefficient with flap deflection for the unswept wing of aspect ratio 3.13 equipped with inboard half-span $\left(b_f = 0.484\frac{b}{2}; \ y_{f_o} = 0.484\frac{b}{2}\right)$ and full-span $\left(b_f = 0.968\frac{b}{2}; \ y_{f_o} = 0.968\frac{b}{2}\right)$ flaps. $y_{f_i} = 0$.
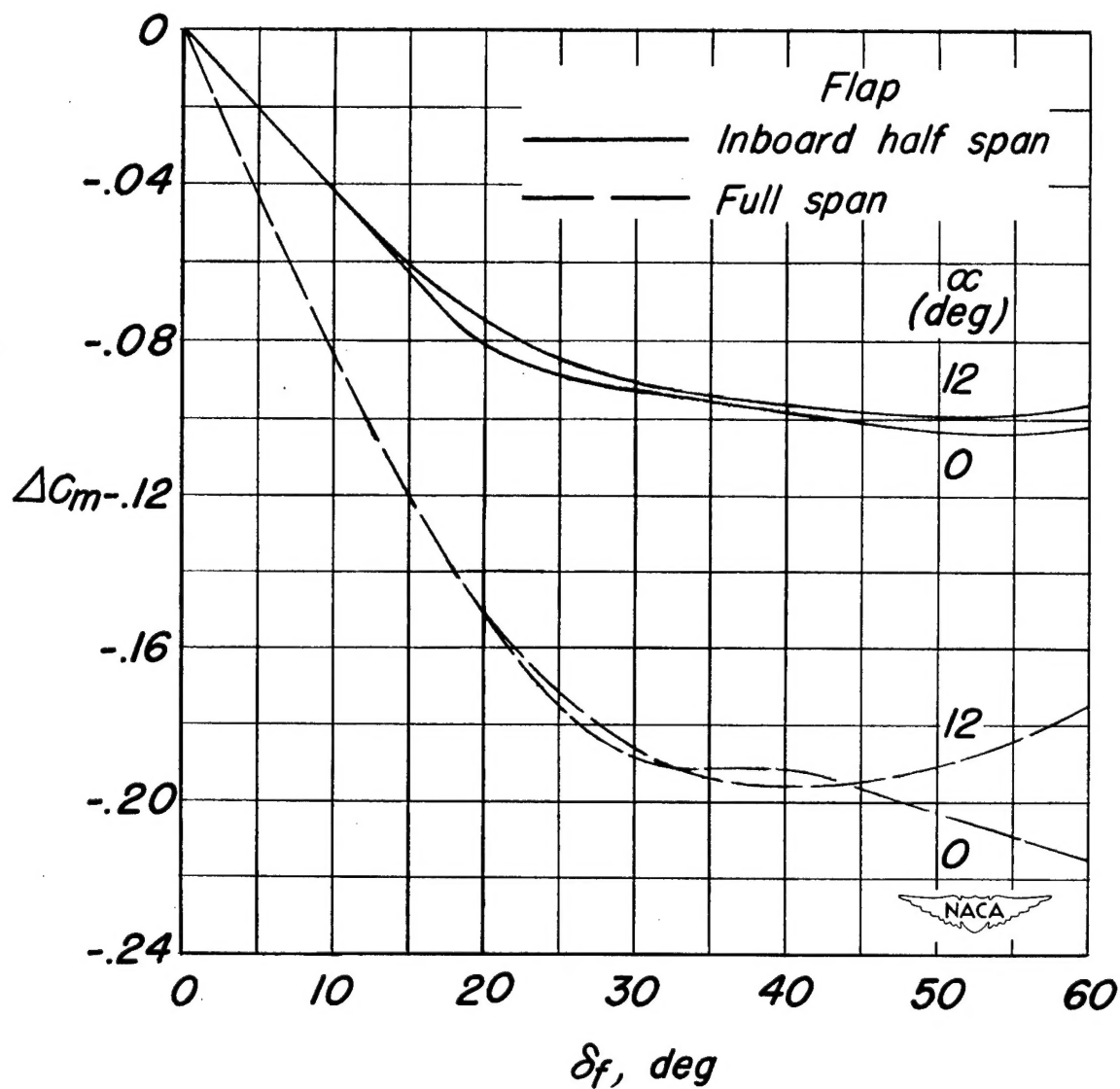
Figure 8.- Variation of incremental pitching-moment coefficient with flap deflection for the unswept wing of aspect ratio 3.13 equipped with inboard half-span $\left(b_f = 0.484\frac{b}{2}; \; y_{f_o} = 0.484\frac{b}{2}\right)$ and full-span $\left(b_f = 0.968\frac{b}{2}; \; y_{f_o} = 0.968\frac{b}{2}\right)$ flaps. $y_{f_i} = 0.$
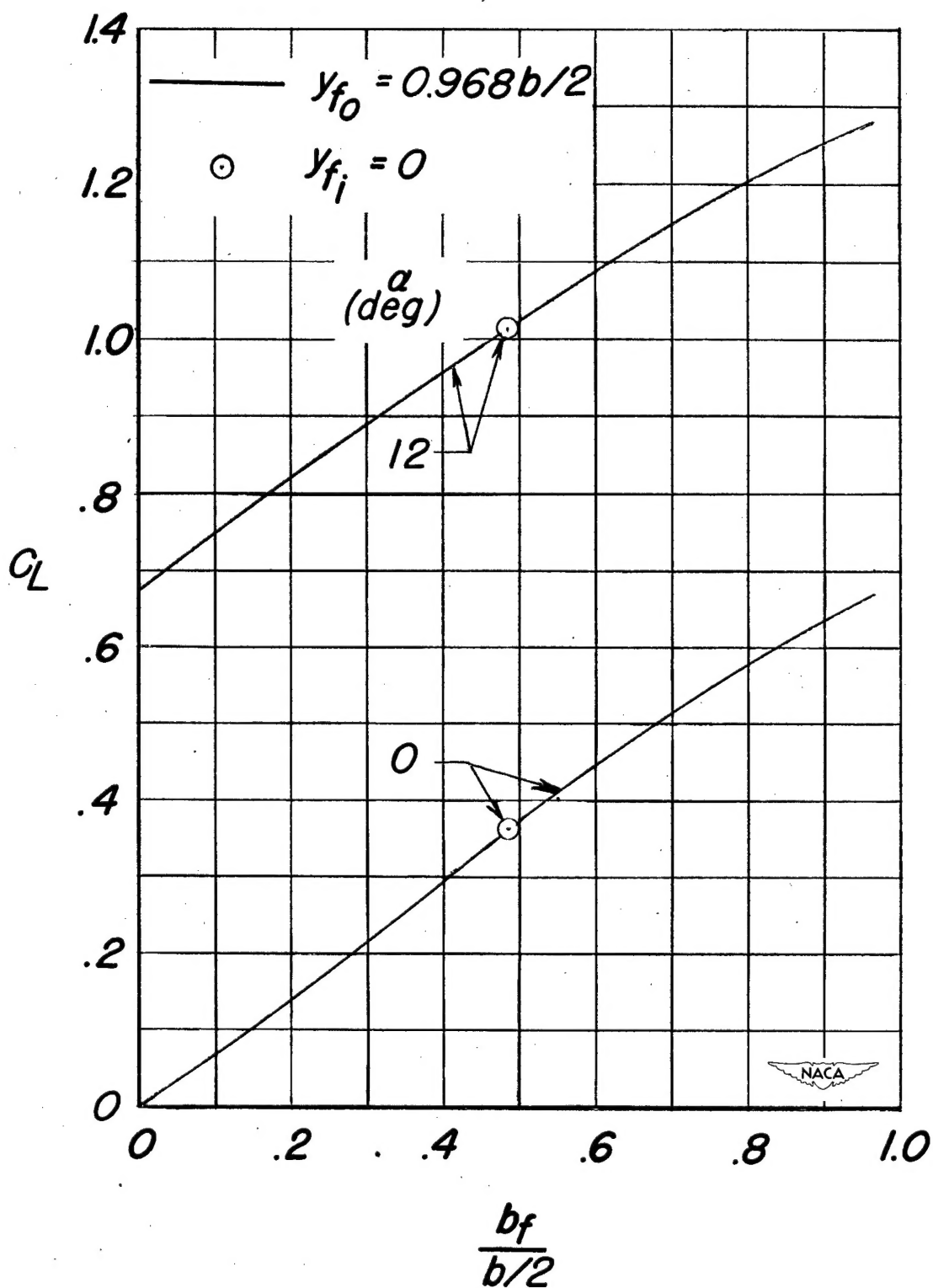
Figure 9.- Effects of flap span and spanwise location on the lift coefficient of the unswept wing of aspect ratio 3.13. $\delta_f = 30°$.

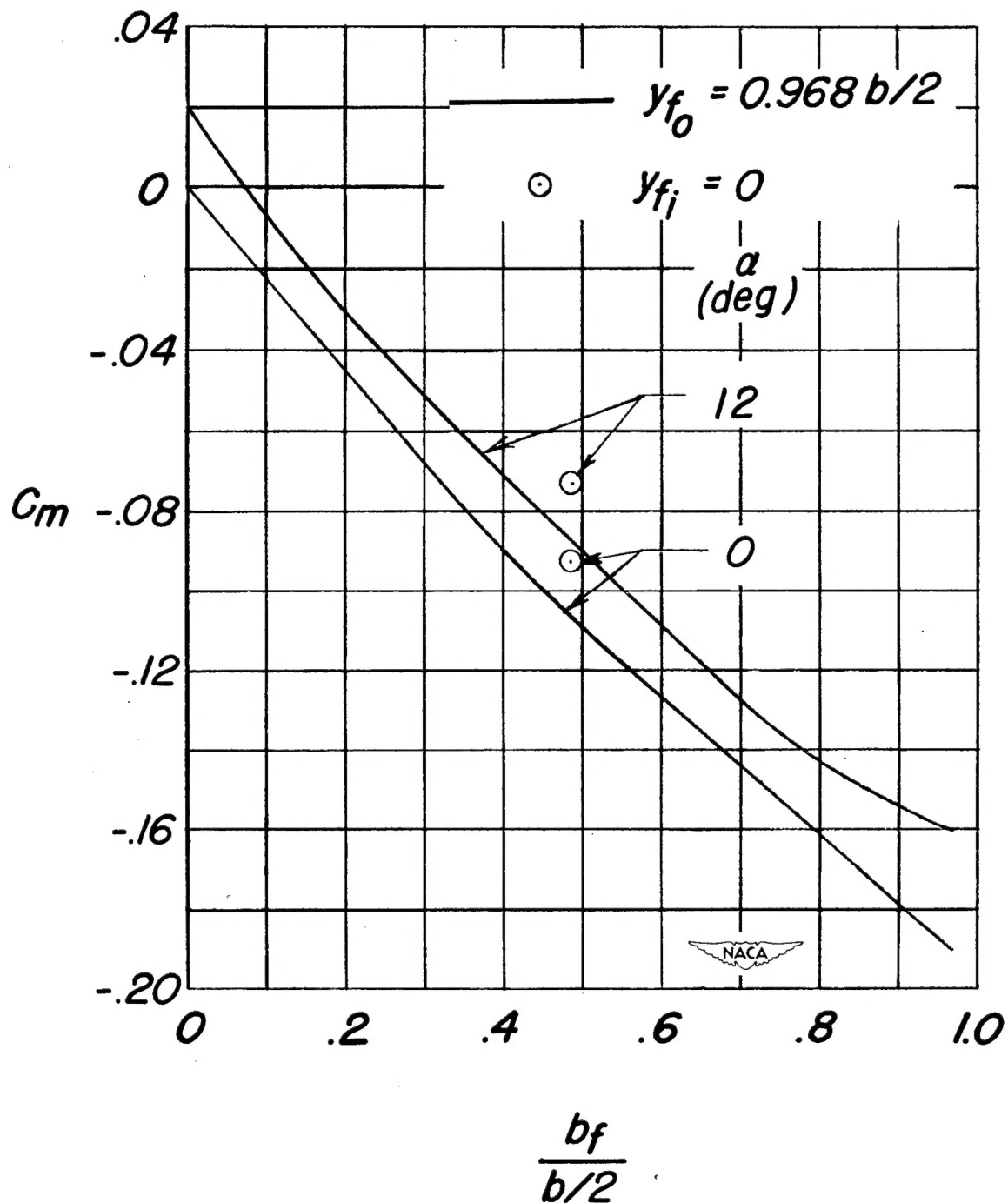Figure 10.- Effects of flap span and spanwise location on the pitching-moment coefficient of the unswept wing of aspect ratio 3.13. $\delta_f = 30°$.

——————Experimental $\dfrac{y_{f_0}}{b/2} = 0.968$

- - - - - Estimated
(reference 10) $\dfrac{y_{f_0}}{b/2} = 1.000$

—— — —Theoretical
(unpublished) $y_{f_i} = 0$
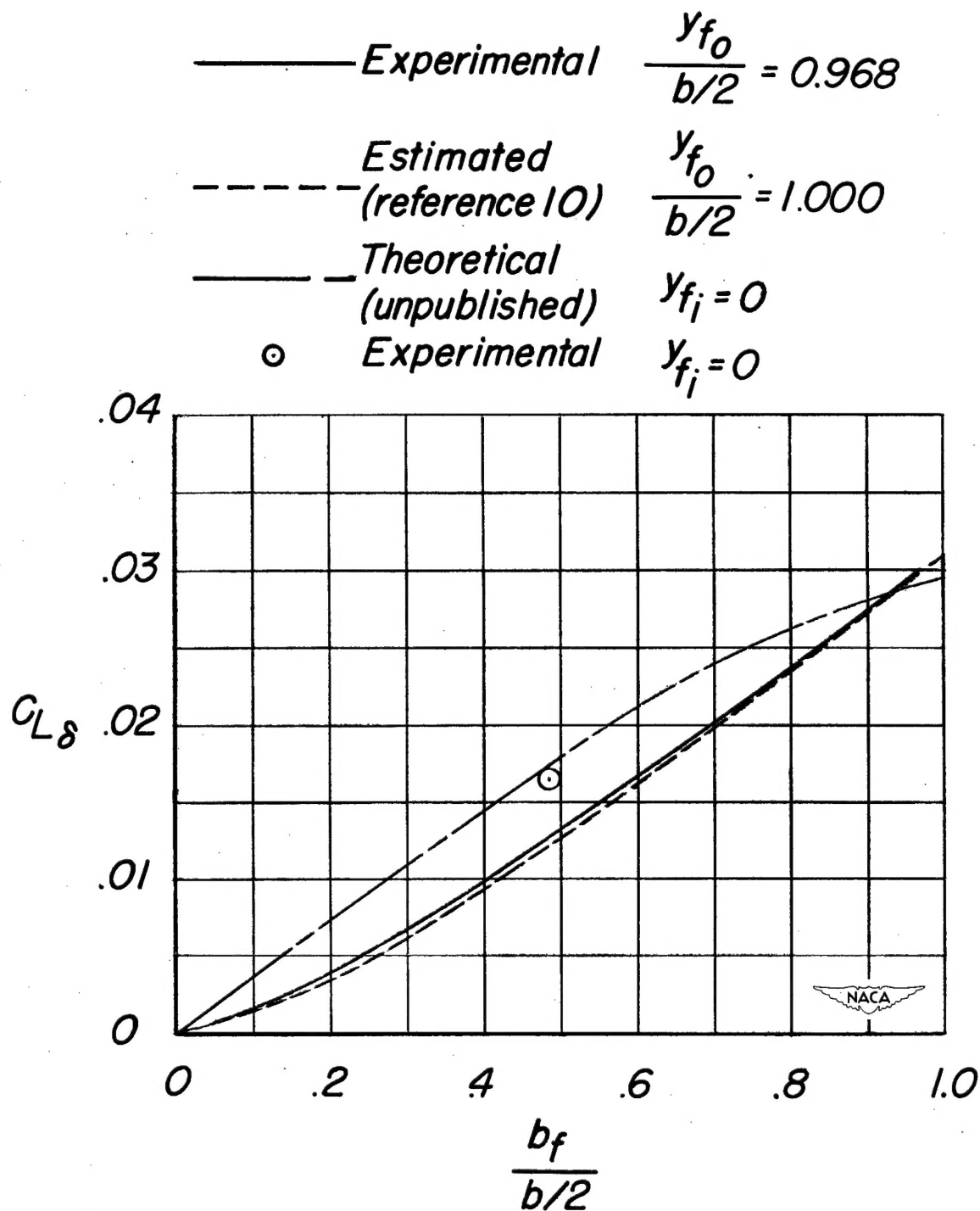
⊙   Experimental $y_{f_i} = 0$

Figure 11.- Effects of flap span and spanwise location on the lift-effectiveness parameter C_{L_δ} of the unswept wing of aspect ratio 3.13.